Salicylic Acid Regulates Plasmodesmata Closure during Innate Immune Responses in *Arabidopsis*[C][W]

Xu Wang,[a] Ross Sager,[a] Weier Cui,[a] Chong Zhang,[b] Hua Lu,[b] and Jung-Youn Lee[a],[1]

[a] Department of Plant and Soil Sciences, Delaware Biotechnology Institute, University of Delaware, Newark, Delaware 19711
[b] University of Maryland Baltimore County, Baltimore, Maryland 21250

ORCID ID: 0000-0003-4604-7974 (J-Y.L).

In plants, mounting an effective innate immune strategy against microbial pathogens involves triggering local cell death within infected cells as well as boosting the immunity of the uninfected neighboring and systemically located cells. Although not much is known about this, it is evident that well-coordinated cell–cell signaling is critical in this process to confine infection to local tissue while allowing for the spread of systemic immune signals throughout the whole plant. In support of this notion, direct cell-to-cell communication was recently found to play a crucial role in plant defense. Here, we provide experimental evidence that salicylic acid (SA) is a critical hormonal signal that regulates cell-to-cell permeability during innate immune responses elicited by virulent bacterial infection in *Arabidopsis thaliana*. We show that direct exogenous application of SA or bacterial infection suppresses cell–cell coupling and that SA pathway mutants are impaired in this response. The SA- or infection-induced suppression of cell–cell coupling requires an ENHANCED DESEASE RESISTANCE1– and NONEXPRESSOR OF PATHOGENESIS-RELATED GENES1–dependent SA pathway in conjunction with the regulator of plasmodesmal gating PLASMODESMATA-LOCATED PROTEIN5. We discuss a model wherein the SA signaling pathway and plasmodesmata-mediated cell-to-cell communication converge under an intricate regulatory loop.

INTRODUCTION

The basal immune response to microbial pathogens requires accumulation of the defense hormone salicylic acid (SA) (Vlot et al., 2009; Rivas-San Vicente and Plasencia, 2011; Fu and Dong, 2013). Plant protein receptors that recognize pathogen-associated molecular patterns or effectors trigger a mitogen-activated protein kinase cascade and a burst of reactive oxygen species that together activate multiple downstream responses (Wiermer et al., 2005; Spoel and Dong, 2012). The core genetic components known to regulate upstream events of SA biosynthesis include *ENHANCED DESEASE RESISTANCE1* (*EDS1*), *PHYTOALEXIN DEFICIENT4*, and *SENESCENCE-ASSOCIATED GENE101* (Wiermer et al., 2005; Dempsey et al., 2011; Rietz et al., 2011). Lipase-like proteins that are encoded by these regulatory genes function together in specific combinations to enhance defense gene expression. Although the underlying molecular mechanisms are not fully known, EDS1 facilitates the expression of *ISOCHORISMATE SYNTHASE1* (*ICS1*), which encodes an SA biosynthetic enzyme that plays a key role in immunity against bacterial infection and other stresses (Wildermuth et al., 2001; Vlot et al., 2009; Dempsey et al., 2011). Following ICS1-based hyperaccumulation of SA, one of the master regulators of SA signal transduction,

NONEXPRESSOR OF PATHOGENESIS-RELATED GENES1 (*NPR1*), is activated by changes in redox conditions within the cell (Tada et al., 2008). As a transcriptional coactivator, NPR1 migrates into the nucleus and brings about major shifts in gene expression patterns, such as induction of pathogenesis-related genes and secretion pathways (Wang et al., 2005; Fu and Dong, 2013).

The critical role of SA as an immune signal has been well documented (Vlot et al., 2009; Rivas-San Vicente and Plasencia, 2011; Fu and Dong, 2013). Direct application of SA activates various pathogenesis-related gene expressions, induces resistance to virulent microbial pathogens, elicits hypersensitive response cell death, and establishes systemic acquired resistance (Malamy et al., 1990; Ryals et al., 1996; Mur et al., 2008; Shah, 2009; Coll et al., 2011). An elegant recent study predicts that a gradient of SA may form such that cells local to the infection site begin hyperaccumulating SA, priming them for cell death, while their neighboring uninfected cells acquire a boost of immunity owing to a lower concentration of SA building up within them (Fu et al., 2012). The molecular mechanisms determining the cellular boundaries between the dying and healthy neighboring cells have yet to be discovered. However, it is conceivable that well-orchestrated local cell communication would be essential in order to confine the hypersensitive response within infected cells so that the detrimental spread of cell death–triggering signals into neighboring healthy cells is prevented (Rustérucci et al., 2001; Rinne and van der Schoot, 2003; Lee and Lu, 2011). In this view, plants would also require a mechanism that coordinates SA-based defense reactions with intercellular connectivity for the full and safe execution of basal immune responses.

Plasmodesmata (PD) allow for direct cytoplasmic connections in the plant and facilitate local molecular exchange among neighboring cells (Robards and Lucas, 1990; Blackman and

---

[C] Some figures in this article are displayed in color online but in black and white in the print edition.

[W] Online version contains Web-only data.

www.plantcell.org/cgi/doi/10.1105/tpc.113.110676

Overall, 2001; Oparka and Roberts, 2001; Cilia and Jackson, 2004; Maule, 2008; Lucas et al., 2009; Burch-Smith et al., 2011; Sevilem et al., 2013). As PDs are initially formed during cell division, virtually all cells are born with plasmodesmal connections with their sister cells by default. However, these primary PD connections are not permanently set for the rest of a cell's life. Rather, they undergo various types of structural modifications and degeneration/regeneration processes to meet the specific needs of cells that may set out rapid expansion, different developmental phases or differentiation, or adaption processes in response to the changes in various physiological and environmental conditions (Ehlers and Kollmann, 2001; Roberts and Oparka, 2003; Lucas and Lee, 2004; Burch-Smith et al., 2011; Burch-Smith and Zambryski, 2012). For instance, PD frequency and density change as cells grow and develop (Gunning, 1978; Seagull, 1983; Ehlers and Kollmann, 1996; Burch-Smith and Zambryski, 2010; Ehlers and van Bel, 2010) or during shifts from vegetative to reproductive phases (Ormenese et al., 2000; Ormenese et al., 2002; Ormenese et al., 2006); PDs differentiate from simple to complex forms (Faulkner et al., 2008; Fitzgibbon et al., 2013); PDs are completely disintegrated during guard cell maturation (Wille and Lucas, 1984); PD permeability undergoes temporal regulation by environmental conditions, such as daylength and temperature (Ormenese et al., 2006; Bilska and Sowinski, 2010; Rinne et al., 2011), etc.

Permeability, dilation, or structure of PDs can be also altered during infection by microbial pathogens (Heinlein, 2002; Benitez-Alfonso et al., 2010; Schoelz et al., 2011; Ueki and Citovsky, 2011). For example, plant viruses spread their infectious materials cell to cell (Benitez-Alfonso et al., 2010) through either regulating PD dilation (Waigmann et al., 1994) or modifying PD structure (van Lent et al., 1991; Pouwels et al., 2003,; 2004). Unlike viruses, bacterial pathogens are mostly epiphytic in their lifestyle, and their mode of infection does not require them to move cell to cell (Hou et al., 2009). However, bacterial infection induces the closure of PD, and a loss of PD regulation or a constitutive closure of PD in *Arabidopsis thaliana* confers either susceptibility or resistance, respectively, to virulent strains of *Pseudomonas syringae* (Lee et al., 2011). We have previously proposed that PLASMODESMATA-LOCATED PROTEIN5 (PDLP5) of *Arabidopsis* acts as a molecular link between the regulation of PD-mediated cell-to-cell coupling and innate immunity (Lee et al., 2011). PDLP5 is a type I transmembrane protein sharing structural and a minimal sequence homology to seven other PD-located proteins (PDLPs) (Thomas et al., 2008). Using immunolocalization in combination with correlative electron microscopy, we mapped the central cavity region as the subdomain of PD that PDLP5 associates with Lee et al. (2011). Interestingly, a recent review reported an immunogold labeling of another PDLP family member, PDLP1, along the length of the PD channel (Maule et al., 2011), which suggests the subdomain of PD that PDLP members are targeted to may not be the same.

More studies are necessary before assigning either specific or redundant functions to each PDLP isoform. However, PDLP5 seems to perform a unique function integral to immune responses among the PDLP isoforms. For example, lack of PDLP5 results in a loss of the regulation of basal PD permeability and an increased susceptibility to bacterial infection, whereas single knockouts of PDLP1, PDLP2, or PDLP3 had no effect on PD permeability (Thomas et al., 2008). PDLP5 alone is transcriptionally and translationally induced by infection with the virulent bacterial pathogen *P. syringae* pv *maculicola* (*Pma*) or by direct application of exogenous SA. The *PDLP5* gene is also called *HOPW1-1-INDUCED GENE1* , which was named based on its transcriptional induction upon infection by *P. syringae* secreting *HOPW1-1* effector (Lee et al., 2008).

Consistent with the finding that *PDLP5* gene induction is regulated by SA, both endogenous and SA-induced expression of *PDLP5* transcript were significantly compromised in *eds1*, *npr1*, and *ics1* mutants (Lee et al., 2011). Moreover, an ectopic overexpression of *PDLP5* induces PD closure, SA accumulation, and basal immunity against virulent bacterial pathogens, whereas the loss-of-function mutant *pdlp5-1* allows for an abnormally extensive PD permeability and enhanced disease susceptibility (Lee et al., 2011). Finally, an introduction of the bacterial gene encoding SA hydroxylase, *NahG*, suppressed the outward plant morphological phenotypes associated with *PDLP5* overexpression, namely, growth retardation and spontaneous lesion development. Taken together, these data indicate that SA accumulation through a positive feedback regulation plays a crucial role in PDLP5 function.

Here, we report that SA signaling components are required to regulate cell-to-cell connectivity as well as the epistatic relationship between the SA pathway and PDLP5. We show that direct application of SA to *Arabidopsis* Columbia-0 (Col-0) induces PD callose deposition and closure, while in the absence of PDLP5, application of exogenous SA was not sufficient to induce these responses. Furthermore, SA mutants defective in SA accumulation or signal transduction are compromised in PD closure upon infection by virulent bacterial pathogens, and the capacity of PDLP5 to activate PD callose deposition and closure is largely dependent on the intact SA biosynthesis and signaling pathway. These results together firmly establish that crosstalk between PDLP5 and the SA pathway is essential for regulating PD permeability during a pathogen defense response.

RESULTS

Direct Application of SA Induces PD Closure

To gain insight into the potential role of SA in modulating cell–cell coupling, we first investigated whether exogenous application of SA has an effect on PD permeability by employing the Drop-and-See (DANS) assay that we developed in a previous study (Lee et al., 2011). The DANS assay uses membrane-permeable, nonfluorescent carboxyfluorescein diacetate as a probe, which acquires fluorescence once released into the cytoplasm through cleavage by cellular esterases and becomes membrane impermeable. The DANS assay has proven to be an effective, noninvasive approach for a real-time, in situ assessment for the extent of molecular diffusion through PD. To test the effect of SA on PD permeability, 3-week-old wild-type Col-0 plants were sprayed with buffer in the absence or presence of SA at 1, 10, or 100 μM, followed by DANS assays on the fourth

and fifth rosette leaves (see Supplemental Figure 1 online). Compared with the buffer control, treating wild-type Col-0 plants with 100 µM SA for 24 h resulted in a significant reduction in PD permeability (Figure 1A). Treating the plants with 100 µM SA for 24 or even for 48 h did not cause any obvious stress or yellowing of the plants. Also, there was no cell death detectable by microscopy (see Supplemental Figure 2 online). Based on these results, we chose to use 100 µM SA and a 24-h time point

as an optimal treatment condition for our study to assess the effect of SA on PD permeability.

SA Accumulation Is Required for PDLP5-Mediated PD Closure

Having found that SA treatment induces PD closure, we then tested whether SA accumulation is required for the reduced PD
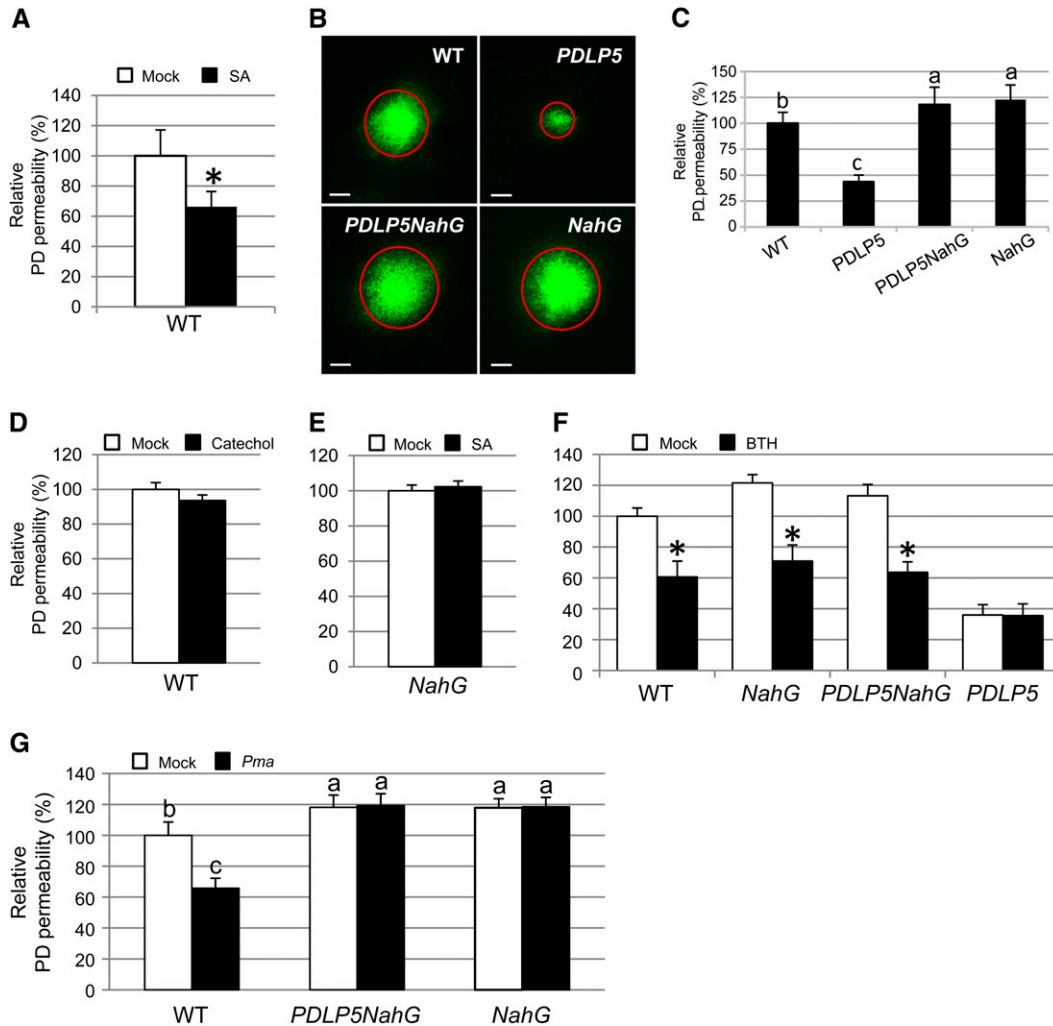

Figure 1. PD Closure Is Regulated by SA.

(A) Relative PD permeabilities of Col-0 plants 24 h after mock treatment or treatment with 100 µM SA. WT, the wild type.

(B) and **(C)** Comparison of PD permeabilities of wild-type Col-0, *PDLP5*, *PDLP5NahG*, and *NahG* plants.

(B) Confocal images showing representative CFDA movement in abaxial leaf surfaces. Circles represent the extent of dye diffusion. Bars = 200 µm.

(C) Quantification of CFDA movement. At least 10 plants were used per assay, and more than three repeats were performed.

(D) to **(G)** DANS assays showing changes in PD permeability in response to various chemicals (100 µM catechol **[D]**, 100 µM SA **[E]**, and 100 µM BTH **[F]**) and pathogen treatments (*Pma ES4326* [OD$_{600}$ = 0.001] **[G]**). Three-week-old plants were sprayed with chemicals or infected with *Pma*. DANS assays were performed at 24 h after treatments by loading CFDA for 5 min on the adaxial surfaces of fourth and fifth leaves and examining the abaxial surface for dye diffusion by a confocal microscopy. At least five individual plants were used per treatment, and two leaves (fourth and fifth) from each plant were subjected to DANS assays. At least two biological repeats were performed for quantification. Asterisks indicate a significant difference (P < 0.001) between two samples. Levels not connected by the same letters are significantly different at the α = 0.05 level according to the LSD test following one-way ANOVA. Bars indicate SE. [See online article for color version of this figure.]

permeability phenotype, which is manifested by transgenic plants overexpressing *PDLP5* under the control of the 35S promoter (hereafter called *PDLP5* plants). To this end, comparative PD permeability assays were performed on 3-week-old wild-type Col-0, *PDLP5*, *NahG*, and homozygous F3 progenies of the cross between *PDLP5* and *NahG* plants (hereafter called *PDLP5NahG*) grown under the same environmental conditions. *NahG* encodes a bacterial SA hydroxylase (Delaney et al., 1994) and was employed as a genetic means to negate SA hyperaccumulation in the *PDLP5* plants. As previously shown in many SA hyperaccumulating mutants (Lorrain et al., 2003; Brodersen et al., 2005), introduction of *NahG* blocked the spontaneous lesion formation phenotype of *PDLP5* plants. Compared with the wild-type Col-0 control, the PD permeability based on the DANS assay is substantially reduced in *PDLP5* (Figures 1B and 1C). However, this PD inhibition phenotype also was completely suppressed by the introduction of *NahG*, indicating that PDLP5 requires SA accumulation to induce the closure of PD.

We predicted that *NahG* would restore the PD permeability in *PDLP5* to a similar level as wild-type Col-0 if *NahG* simply eliminates the *PDLP5*-induced SA hyperaccumulation. Surprisingly, *PDLP5NahG* exhibited greatly enhanced PD permeability, allowing for ~20% higher diffusion of the fluorescent reporter than the wild type (Figures 1B and 1C). Notably, this level of extensive PD permeability was previously observed in *pdlp5-1* (Lee et al., 2011). The level of *PDLP5* transcript in *PDLP5NahG* was comparable to that in the parental line *PDLP5* (Lee et al., 2011), eliminating the possibility that the restored PD permeability in *PDLP5NahG* may reflect a potential fluctuation or instability in *PDLP5* expression. Thus, the enhanced PD permeability in *PDLP5NahG* led us to ask whether the overexpression of *NahG* alone could enhance PD permeability. Indeed, subsequent DANS assays on *NahG* plants revealed that an overexpression of *NahG* alone can significantly enhance the dye diffusion through PD (Figures 1B and 1C). Fluorescent dye absorption on the adaxial surface in transgenic or mutant lines was comparable to that in wild-type plants, as we had shown previously for the *PDLP5* and *pdlp5-1* (Lee et al., 2011; see Supplemental Figure 3A online). In addition, overall epidermal cell sizes on both adaxial and abaxial sides of *PDLP5*, *NahG*, and *PDLP5NahG* were comparable to those of wild-type Col-0 plants (see Supplemental Figures 3B and 3C online). Thus, the aberrant PD permeability shown in *NahG* or *PDLP5NahG* was apparently not due to an alteration in epidermal surface property or cell size.

The ability of *NahG* to suppress the phenotypes associated with SA hyperaccumulation has been largely attributed to its SA hydroxylase activity, which disables SA accumulation (Lawton et al., 1995). However, there was a report that a certain phenotype manifested by the introduction of *NahG* is linked to an inappropriate production of an SA degradation by-product, catechol (van Wees and Glazebrook, 2003). We therefore tested the possibility that the enhancing effect *NahG* has on PD permeability is linked not necessarily to the lack of SA accumulation, but rather to an increased catechol production. The DANS assays performed 24 h after spraying wild-type Col-0 with 100 μM catechol (van Wees and Glazebrook, 2003) demonstrated that this catechol treatment has no effect on the PD permeability

(Figure 1D). These results indicate that the inability to accumulate SA, rather than catechol accumulation, attributes to extensive opening of PD in *NahG* plants.

In contrast with the repressive effect of SA on symplastic dye diffusion in wild-type Col-0 (Figure 1A), the same SA treatment failed to induce PD closure in *NahG* (Figure 1E), as expected. However, application of an SA agonist, benzo(1,2,3) thiadiazole-7-carbothioic acid (BTH), which is not degradable by *NahG*, could induce PD closure in *NahG* to a similar extent shown in BTH-treated wild-type plants (Figure 1F). Moreover, BTH treatment could restore the reduced PD permeability phenotype in *PDLP5NahG*, whereas such treatment did not have any additional effect in *PDLP5* plants. Collectively, our data provide strong experimental evidence that SA both acts as a signal to restrict cell-to-cell coupling and is required for PDLP5-mediated PD closure.

Inability to Accumulate SA Leads to the Loss of the Regulation of PD during Defense

In response to virulent *Pma* infection, cell-to-cell diffusion through PD becomes highly restricted in *Arabidopsis* Col-0 (Lee et al., 2011). Having established that exogenous application of SA promotes PD closure, we speculated that the *Pma*-induced PD closure might also be attributed to cellular activation of SA biosynthesis and accumulation resulting from innate immune responses. To test this hypothesis, the PD permeability of *NahG* upon *Pma* infection was examined in comparison to Col-0 wild-type plants; we reasoned that the inability to accumulate SA would make *NahG* insensitive to *Pma* infection in terms of the PD response. Indeed, we found that bacterial infection failed to induce PD closure in *NahG* as well as in *PDLP5NahG*, while infected wild-type Col-0 exhibited a substantial reduction in PD permeability compared with the mock-treated plants (Figure 1G). The SA deficiency in *PDLP5NahG* also suppressed the *PDLP5* pathogen-resistant phenotype, indicating that SA buildup is in fact required for both the regulation of PD and basal immunity in *PDLP5* plants. These results underscore the dual role of SA as a hormonal signal that not only activates defense but also regulate symplastic cell-to-cell connectivity during the plant response to microbial pathogens.

SA Induces PD Callose Deposition

Pma infection was previously found to stimulate callose deposition at PD (Lee et al., 2011), but at that time, it was unknown which signaling molecules or pathway regulated that response. However, in light of the results described above, it seemed prudent to test the possibility that callose deposition restricting PD during the defense response to *Pma* was also regulated by SA. To this end, we examined the effect of SA on PD callose deposition by treating 3-week-old Col-0 plants with 100 μM SA spray for 24 h, followed by aniline blue staining for callose detection in the rosette leaves and quantification of the fluorescence foci intensity per square micron. Compared with the mock control, the leaves treated with SA accumulated over twofold higher PD callose (Figure 2A). This result together with the finding that PD permeability is highly enhanced in *NahG*

suggested that a lack of SA accumulation may avert deposition of PD callose in *NahG*. Indeed, the basal PD callose deposition in *NahG* was substantially lower, comprising only 30% of the wild-type level (Figure 2B). Moreover, consistent with the suppressive effect of *NahG* on the reduced PD permeability phenotype of *PDLP5*, *NahG* also eliminated the phenotype of *PDLP5* associated with hyperaccumulation of PD callose (Figure 2C). These data support the idea that SA is a crucial hormonal factor regulating cell-to-cell permeability via recruiting callose to PD.

SA Does Not Rescue the Enhanced PD Permeability Phenotype of *pdlp5-1*

Since a high *PDLP5* expression level within cells stimulates SA accumulation, one could argue that the restricted PD phenotype

of *PDLP5* is due simply to SA hyperaccumulation triggering closure through another, PDLP5-independent mechanism. If this were indeed true, then supplying *pdlp5-1* with exogenous SA would induce a near *PDLP5*-level of PD closure because the loss of PDLP5 would not stop SA from exerting its PD-closing function. To test this possibility, we performed DANS assays on Col-0 and *pdlp5-1* that were either mock treated or treated with 100 µM SA. In stark contrast with the wild-type control, the SA-induced PD closure response was fully impaired in *pdlp5-1*, which retained a higher PD permeability even in the presence of exogenously supplied SA (Figures 3A and 3B). We next addressed whether PDLP5 was essential for closing PD during a response to bacterial pathogen by performing DANS assays on *pdlp5-1* following *Pma* infection. This experiment showed that *Pma*-induced PD closure is also fully impaired in *pdlp5-1* (Figure 3C). This result, together with the loss of SA sensitivity
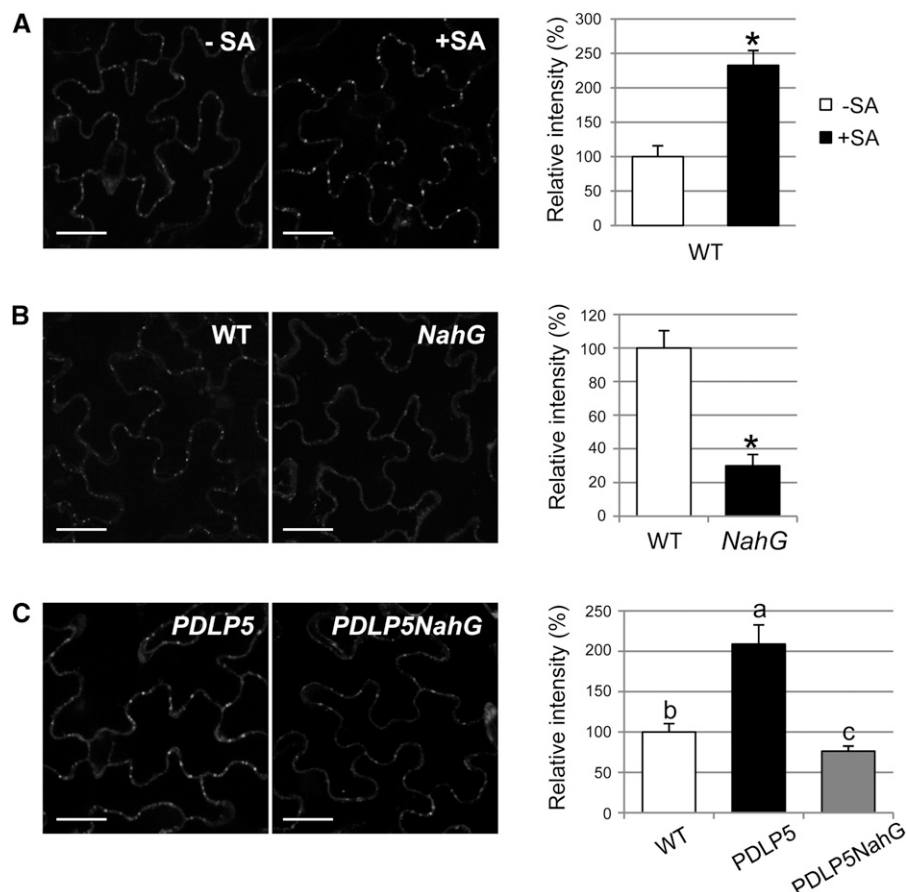

Figure 2. PD Callose Deposition Is Dependent on SA Accumulation.

(A) Confocal images showing callose staining at PD (left panels) and quantification of PD callose level (right) in wild-type (WT) Col-0 mock treated (-SA) or treated with 100 µM SA (+SA). Abaxial surfaces of the fourth and fifth leaves of 3.5-week-old plants were imaged by a confocal microscopy following aniline blue staining. Bars = 20 µm.

(B) Callose level in *NahG* compared with wild-type plants.

(C) Suppression of PD callose accumulation in *PDLP5* by *NahG*. At least three individual plants were used per treatment and fourth and fifth leaves from each plant were subjected to aniline blue staining. Two biological repeats were performed for quantification. Asterisks indicate a significant difference ($P < 0.0001$) between two samples by t test. Levels not connected by same letters are significantly different at the $\alpha = 0.05$ level based on LSD test following one-way ANOVA. Bars indicate SE.
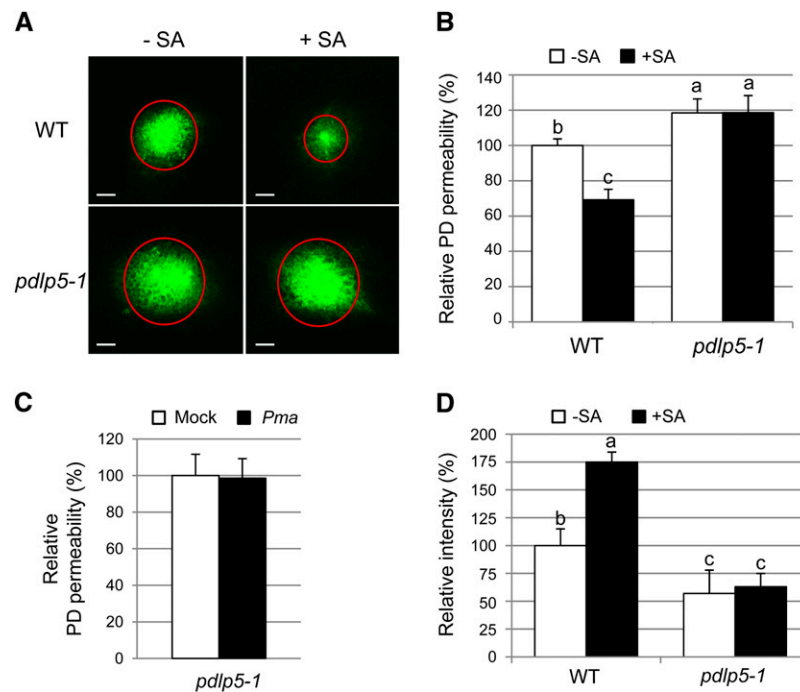
Figure 3. PDLP5 Is Essential for SA-Induced PD Closure and Callose Deposition.

(A) to **(C)** DANS dye loading assays showing impairment of induced PD closure response in *pdlp5-1* upon either 100 μM SA treatment ([**A**] and [**B**]) or *Pma* infection **(C)**. Representative confocal images of abaxial leaf surfaces show the effects of SA treatment on the extents of dye diffusion **(A)**. WT, the wild type. Bars = 200 μm.

(D) Lack of SA-induced PD callose accumulation in *pdlp5-1*. More than five and three individual plants were used for DANS assays and aniline blue staining, respectively. At least two biological repeats were performed for quantification. All images were taken from leaf number 4 and leaf number 5. Levels not connected by same letters are significantly different at the α = 0.05 level based on LSD test following one-way ANOVA. Bars indicate SE. [See online article for color version of this figure.]

demonstrated in *pdlp5-1* (Figures 3A and 3B), indicates that PDLP5 is indeed a key molecular player for translating SA signaling to PD closure during defense responses. Collectively, our data provide strong experimental evidence that PDLP5 and SA exert their effect on PD in an interdependent manner such that restriction of PD requires both components.

PDLP5 Is an Essential Molecular Link between the SA-Based Defense Response and PD Callose Deposition and Closure

Numerous reports have presented a correlation between PD closure and callose deposition (Radford et al., 1998; Simpson et al., 2009; Lee et al., 2011; Vatén et al., 2011; Zavaliev et al., 2011; Koh et al., 2012), supporting the general consensus that enhanced PD callose deposition is indicative of PD closure and, thus, inhibition of cell-to-cell coupling. Our study has shown that the relative amount of PD callose deposition is inversely correlated with the extent of PD permeability but directly correlated with the level of *PDLP5* expression (Lee et al., 2011). However, it was unclear to us whether the increase in PD callose level during infection was also dependent on PDLP5 or any other factors (such as SA hyperaccumulation). We addressed this question by examining PD callose levels in *pdlp5-1* following application with

exogenous SA. If *pdlp5-1* responds normally to the SA treatment in terms of elevated PD callose level, it would mean that SA, not PDLP5, is responsible for augmenting PD callose. However, while wild-type Col-0 responded to exogenous SA by inducing a significant amount of PD callose deposition, this response was also fully impaired in *pdlp5-1* (Figure 3D). This result confirms that the induced PD callose response upon SA accumulation is indeed dependent on PDLP5, further supporting that PDLP5-mediated PD closure is most likely mediated through callose deposition at PD.

SA Defense Pathway Mutations Are Epistatic to PDLP5

Based upon the data described above, it is clear that SA regulates PD permeability in conjunction with PDLP5. To gain further insight into the functional relationship between PDLP5 and SA, we determined epistatic relationships between the genetic components of SA pathway and PDLP5 using *PDLP5* and SA mutants. We chose the SA mutants *eds1-2*, *ics1-1*, and *npr1-1*, which lack the key upstream regulator of SA signaling pathway EDS1, SA biosynthetic enzyme ICS1, and SA downstream regulator NPR1, respectively (Cao et al., 1994; Aarts et al., 1998; Wildermuth et al., 2001). We isolated homozygous F3 progenies of *PDLP5eds1*, *PDLP5ics1*, and *PDLP5npr1* and then examined

which genetic mutations can suppress the PD permeability phenotype in *PDLP5*. The homozygosity of the SA pathway mutations and the homogeneous *PDLP5* expression level in those double mutants were confirmed by transcript analysis using RT-PCR (see Supplemental Figure 4A online). Morphological comparisons of *PDLP5eds1*, *PDLP5 ics1*, and *PDLP5 npr1* to the *PDLP5* parental line showed that all three mutations suppressed the stunted growth phenotype of *PDLP5* to a certain extent (Figure 4A). Furthermore, the highly elevated SA level found in the *PDLP5* parental line was also diminished (Figure 4B), with a subsequent reduction or abolition of the SA hyper-accumulation marker *PR1* (see Supplemental Figure 4B online), confirming that abnormal induction of *PR1* in *PDLP5* depends on these genetic components. These results indicate that PDLP5-regulated positive SA feedback must work through the basal SA defense pathway components EDS1, ICS1, and NPR1.

We next examined PD permeability phenotype in *PDLP5eds1*, *PDLP5ics1*, and *PDLP5npr1*. Fluorescent dye absorption on the adaxial surface and overall epidermal cell sizes on both adaxial and abaxial sides in SA mutants and crosses were comparable to those in wild-type plants (see Supplemental Figure 3 online). Subsequent DANS assays on these plants demonstrated that all three mutations were able to suppress the restricted PD permeability in *PDLP5* (Figure 4C). However, whereas both *eds1* and *npr1* were able to fully suppress the reduction in PD permeability, *ics1* was only partially effective. This result suggests that PDLP5-mediated PD closure requires an EDS1- and NPR1-dependent SA pathway.
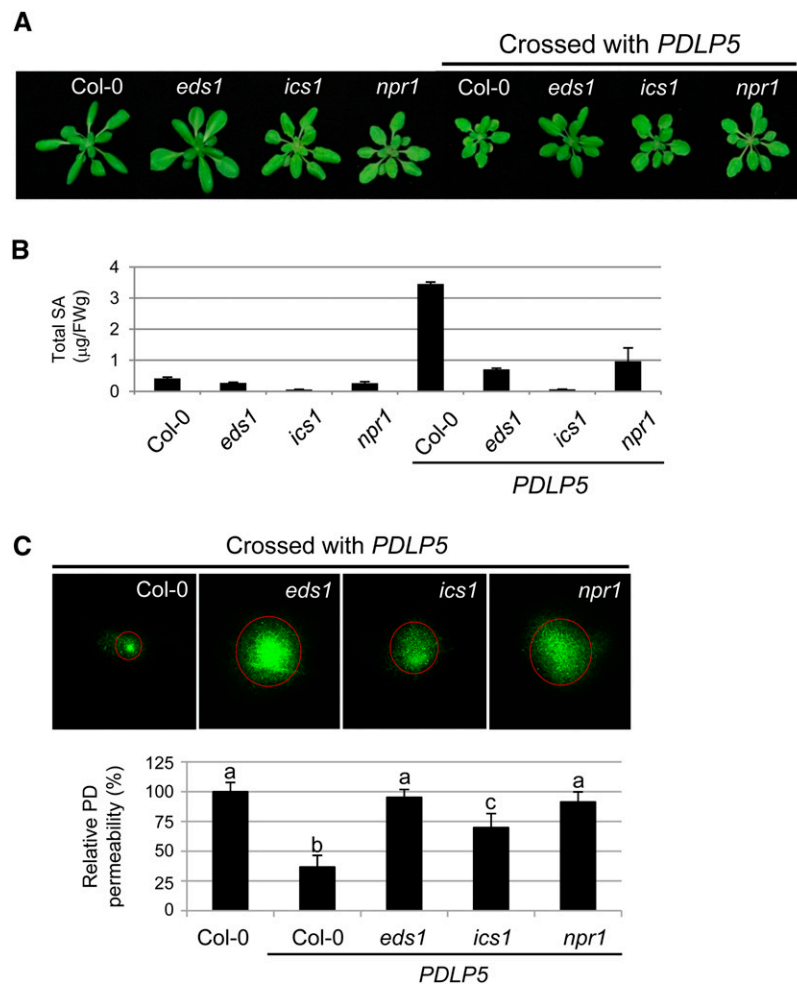

Figure 4. SA Mutants Are Epistatic to *PDLP5*.

(A) Morphologic phenotypes of *eds1*, *ics1*, *npr1*, and their crosses with *PDLP5*: *PDLP5eds1*, *PDLP5ics1*, and *PDLP5npr1*, respectively.

(B) Total SA levels in each genetic background.

(C) DANS assays showing PD permeability in SA mutants in *PDLP5* background along with wild-type control. Representative confocal images of abaxial leaf surfaces are shown. For each genetic background, at least five individual plants were used for DANS assays with at least two biological repeats. Levels not connected by same letters are significantly different at the $\alpha = 0.05$ level based on the LSD test following one-way ANOVA. Bars indicate SE.

[See online article for color version of this figure.]

Basal PD Permeability Is Normal in SA Mutants

Considering a potential mechanism by which SA acts on PD, we propose two simple possibilities. One is that SA is a chemical agonist that directly affects PDLP5 or other PD components. The other is that SA acts indirectly as a hormonal signal that activates a downstream signaling pathway (s) on which PDLP5 activity/function relies. To gain insight into the mechanistic relationship between SA and PD permeability, we decided to investigate the latter possibility by examining PD permeability phenotypes of SA mutants. To this end, basal PD permeability was first measured by performing DANS assays on the SA pathway mutants *eds1*, *ics1*, and *npr1*. This test showed that the basal level of PD opening in these mutants under normal growth conditions was comparable to that of wild-type controls (Figures 5A and 5B). Notably, *eds1* showed a slightly lower PD permeability than wild-type Col-0, a result that was perplexing considering the endogenous SA level in this mutant was lower than Col-0 (Figure 4B). Since *eds1* is derived from the Landsberg *erecta* (L*er*) ecotype, we subsequently tested whether the low PD permeability detected in *eds1* reflects a difference between L*er* and Col-0 ecotypes. Indeed, the DANS assay showed that wild-type L*er* plants exhibited slightly lower PD permeability compared with wild-type Col-0, and the PD permeability of *eds1* was comparable to wild-type L*er* (Figure 5C).

Induced PD Closure Response Is Compromised in SA Mutants

Since *NPR1* is the most downstream regulator, responsible for regulating many of the critical genetic responses to SA accumulation during defense (Wang et al., 2005), we decided to determine if *NPR1* was also essential for regulating the pathogen-induced reduction in PD permeability. Indeed, the PD closure response normally induced by *Pma* infection was fully impaired in the absence of functional NPR1 either in wild-type or *PDLP5* backgrounds (Figure 6A). Furthermore, quantitative analyses of aniline blue–stained PD callose revealed that basal PD callose levels in the wild type and *npr1-1* were comparable to each other. However, the loss of NPR1 could fully suppress the hyper PD callose accumulation phenotype in *PDLP5npr1* (Figure 6B). These data establish the dependence of PDLP5 on NPR1 in modulating PD callose accumulation and, hence, PD closure during immune responses.

Although signaling downstream of SA is largely dependent on *NPR1*, some SA responses are *NPR1* independent (Ferrari et al., 2003; Blanco et al., 2005). To determine whether SA-induced PD closure relies solely on an *NPR1*-dependent pathway, we performed additional DANS assays using *npr1* and *PDLP5npr1* following SA application. This experiment showed that exogenous SA application was not able to complement the loss of NPR1 (Figure 6C), thus validating that SA-induced PD closure requires *NPR1* or its downstream factor(s). By contrast, SA application restored normal PD closure response in *PDLP5eds1* and *PDLP5ics1* (see Supplemental Figure 5 online).

In conclusion, we demonstrated that SA is a critical signaling molecule for regulating cell-to-cell connectivity and that SA-directed PD closure requires PDLP5 as the molecular link between the SA pathway and PD modulation. PDLP5 functions to close PD during immune responses by working simultaneously with an *NPR1*-dependent pathway to trigger a high level of callose deposition at PD during infection. And without either PDLP5 or NPR1, *Arabidopsis* cannot close PD in response to pathogen infection.
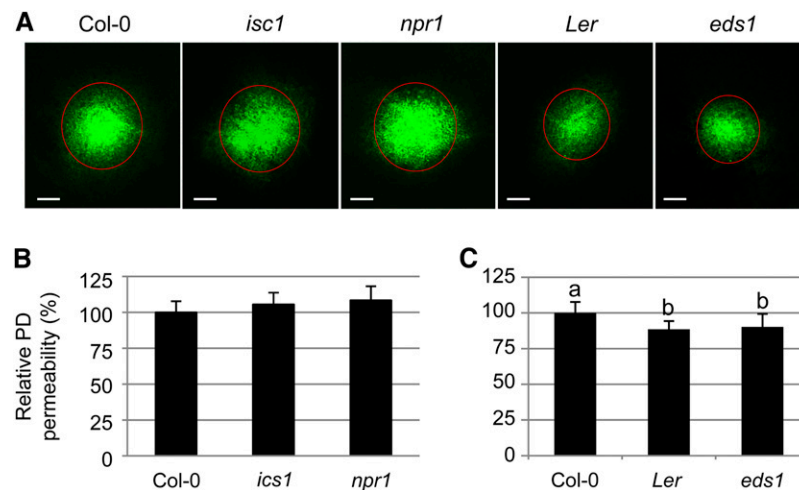

Figure 5. Basal PD Permeability in SA Mutants Is Normal.

(A) Representative confocal images of abaxial leaf surfaces showing basal PD permeability in Col-0, *ics1*, *npr1*, L*er*, and *eds1*. Bars = 200 μm.
(B) and **(C)** Quantitative comparison of PD permeability in *ics1* and *npr1* compared with wild-type Col-0 **(B)** and *eds1* compared with wild-type L*er* **(C)**. For each genetic background, at least five individual plants were used for DANS assays with at least two biological repeats. Levels not connected by same letters are significantly different at the α = 0.05 level based on LSD test following one-way ANOVA. Bars indicate SE.
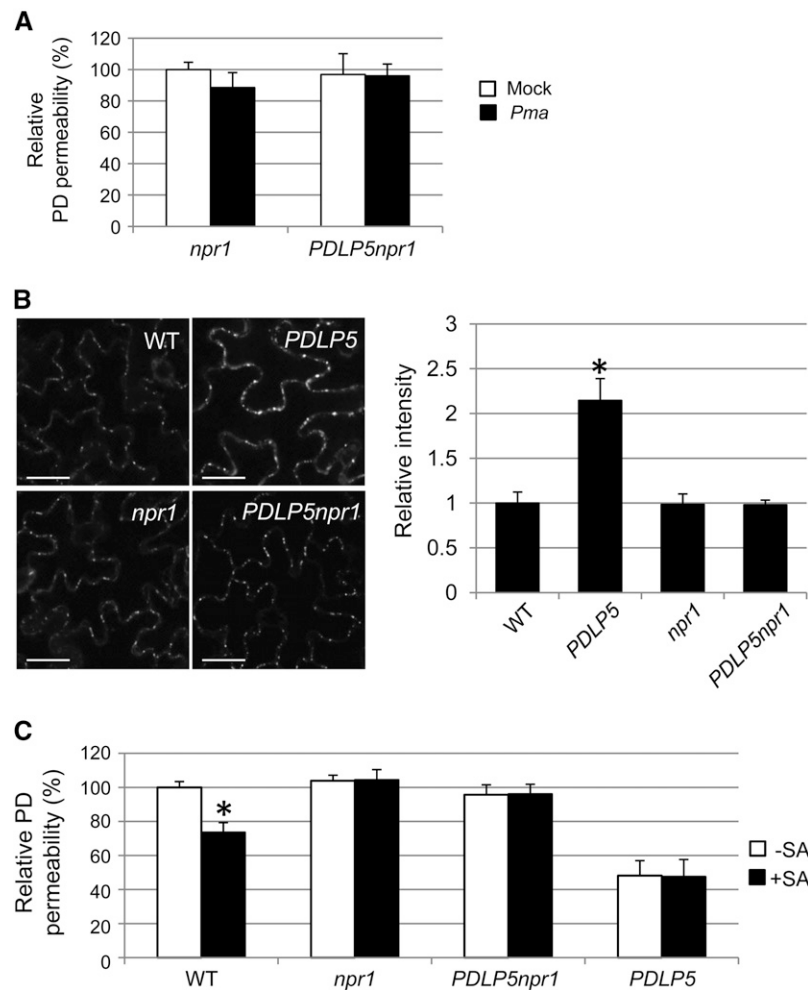[See online article for color version of this figure.]

Figure 6. NPR1 Is Required for PDLP5-Mediated PD Closure and Callose Deposition.

(A) Lack of PD closure response in *npr1* and *PDLP5npr1* to *Pma* infection.

(B) Basal PD callose level in *npr1* and *PDLP5npr1* is normal. Abaxial surfaces of the fourth and fifth leaves of 3.5-week-old plants were imaged by a confocal microscopy following aniline blue staining. WT, the wild type. Bars = 20 μm.

(C) PD permeability in *npr1*, *PDLP5npr1*, and *PDLP5* is insensitive to 100 μM SA treatment. More than five and three individual plants were used per treatment for DANS assays and aniline blue staining, respectively. At least two biological repeats were performed for quantification. Asterisks indicate a significant difference (P < 0.001) between two samples by *t* test.

DISCUSSION

We had shown in a recent study that the SA pathway plays a role in regulating PD by upregulating a PD inhibitor, PDLP5, during immune responses against bacterial pathogens (Lee et al., 2011). In this article, we provided experimental evidence supporting that an accumulation of SA is critical to block PD in *Arabidopsis* and established an epistatic relationship between SA biosynthetic/signaling components and PDLP5. First, exogenous application of SA or BTH induces PD callose deposition, which results in PD closure. Second, defects in SA accumulation or signaling in *NahG* and *npr1*, respectively, compromise the ability to close PD in response to either SA treatment or bacterial infection. Third, in the absence of PDLP5, plants were also not able to stimulate PD callose deposition; thus, there was no PD closure after treatment with exogenous SA or during bacterial infection. Finally, dissection of epistatic relationships revealed that the physiological and cellular phenotypes associated with overexpression of PDLP5, such as SA hyperaccumulation, increased PD callose deposition, and severe restriction of PD permeability, are suppressed in *eds1*, *ics1*, *npr1*, and *NahG*. Taken together, these data provide insight into how PD closure is regulated during defense. Namely, bacterial pathogen infection triggers the basal SA defense pathway, and SA accumulation activates both NPR1 and PDLP5, which must work in tandem to produce a complete PD closure response, via increasing PD callose deposition. This response is reinforced by a positive feedback loop through the SA defense pathway, which requires the components EDS1, ICS1, and NPR1 (Figure 7).

SA Accumulation via ICS1 Is Required but Not Sufficient for PDLP5-Mediated PD Closure

In *Arabidopsis*, SA is synthesized primarily via the isochorismate-using pathway in the chloroplast and secondarily via the Phe ammonia-lyase pathway. ICS1, a biosynthetic enzyme in the isochorismate pathway, is not required for the maintenance of the basal level of SA but is mainly responsible for SA accumulation during bacterial infection (Wildermuth et al., 2001). Interestingly, the SA levels in *PDLP5eds1* and *PDLP5npr1* are elevated but are not as high as in the *PDLP5* parental line. By contrast, *PDLP5ics1* was found to have a similar SA level to that of *ics1* alone (Figure 4B), which indicates that SA accumulation in *PDLP5* is fully dependent on ICS1 function. However, while the basal PD permeability of *eds1*, *ics1*, and *npr1* was no different from that in each of their wild-type ecotypes (either Col-0 or L*er*; Figure 5), both the *eds1* and *npr1* mutations fully suppressed *PDLP5*-induced PD closure, whereas *ics1* could only partially suppress the PDLP5-restricted PD phenotype (Figure 4C). These data suggest the presence of an additional factor(s) independent of ICS1-amplified SA that is responsible for PD closure via PDLP5 through EDS1- or NPR1-triggered changes in defense signaling. We speculate that factors from both ICS1-dependent and -independent pathways may work together to produce the maximum activity/function of PDLP5.

Do SA and PDLP5 Impede Dye Movement through Induction of Cell Death or PD Modification?

We have shown in our previous study that overexpression of PDLP5 results in hyperaccumulation of SA and spontaneous lesions (Lee et al., 2011). It is possible that cell death might have impeded dye movement in *PDLP5* plants to some extent apart from or in addition to PD callose deposition. The *PDLP5* line
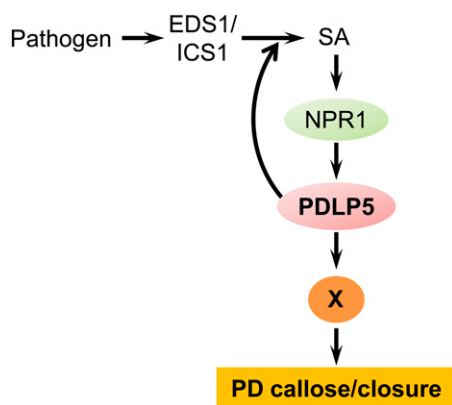

Figure 7. An Illustrated Model Demonstrating the Crosstalk between *PDLP5*-Mediated PD Regulation and SA Defense Signaling.

Pathogen infection induces *PDLP5* expression via an EDS1/ICS/NPR1-dependent SA pathway. A positive feedback loop between *PDLP5* and SA accumulation requires EDS1, ICS1, and NPR1. Hyperaccumulation of PDLP5 leads to callose-dependent PD closure. This PDLP5 function requires NPR1, perhaps via a yet unknown "factor X."
[See online article for color version of this figure.]

used in this study was an intermediate line that has a mild cell death phenotype. Moreover, cell death in *PDLP5* plants progresses with aging, becoming visible at 4 to 5 weeks after germination starting from the edges of the oldest leaves. All our DANS assays and callose staining were done on the central regions of the fourth and fifth rosette leaves of 3-week-old plants, in which there are few to no lesions. Also, treatment with 100 µM SA for 24 h or longer did not cause lesions to form but still resulted in a reduction in PD permeability. Based on these pieces of circumstantial evidence, it appears that cell death might be a later response than or eventual outcome of PD closure.

What might be the direct role that SA and SA pathways play in regulating PD? Could SA affect the subcellular localization of PDLP5? We tested this possibility, but PDLP5 localization at PD remained the same 24 or even 48 h after SA treatment (see Supplemental Figure 6 online). It is possible that SA or SA pathways may induce a component that PDLP5 requires for its function; our data indicate that PDLP5 cannot function to close PD in the absence of this SA-dependent component, factor X (Figure 7). SA was shown to facilitate secondary PD formation in *Arabidopsis* seedlings grown on SA-containing medium for several days (Fitzgibbon et al., 2013). It would be interesting to determine whether there is a close link between structural modification of PD and the SA pathway during immune responses and whether SA together with PDLP5 induces PD closure through such modification.

Basal PD Callose/Permeability Requires SA in Conjunction with PDLP5 but Not npr1

In contrast with *ics1*, *NahG* fully suppressed the restricted-PD phenotype in *PDLP5*. This result is not too surprising, as several previous reports have documented that *NahG* and *ics1* do not always suppress phenotypes associated with SA hyperaccumulation in a similar manner (Nawrath and Métraux, 1999; Heck et al., 2003; Brodersen et al., 2005; Jagadeeswaran et al., 2007; Vogelmann et al., 2012). One obvious possibility is that *NahG* is more efficient at eliminating SA in the *PDLP5* background than *ics1*, considering their efficacies in suppressing the *PDLP5* phenotype. Along this line, we could argue that SA is the major factor PDLP5 requires to close PD and that SA synthesized independently of ICS1 might play a role in both maintaining basal PD permeability and responding to pathogen infection. Thus, *NahG* is more potent than *ics1* in suppressing *PDLP5* because it degrades SA from all sources within the plant, while *ics1* only prevents ICS1-dependent SA accumulation. Consistent with this idea, treating *NahG* plants with nondegradable SA analog BTH induced PD closure, as was also the case for BTH-treated wild-type plants.

While the highly enhanced basal PD permeability in the *NahG* background was not seen in *ics1*, *eds1*, or *npr1*, the permeability observed in the *NahG* background was quite similar to that in *pdlp5-1* (Figure 3). An intriguing question here is whether there is a common factor that *NahG* and *pdlp5-1* share to open PD beyond the basal level. One may logically suggest that the enhanced PD permeability in *pdlp5-1* has to do with greatly reduced or eliminated SA, similar to *NahG*. However, our previous study has already shown that the SA content in *pdlp5-1* was not

different from that in the wild type (Lee et al., 2011), under-scoring that a loss of PDLP5 results in an enhancement in basal PD permeability regardless of having a normal SA level. Another possibility is that there is not sufficient SA in the *NahG* plants to maintain normal levels of *PDLP5*. Indeed, RT-PCR data show that the *PDLP5* expression level in *NahG* is lower than that in *ics1* and the wild type (see Supplemental Figure 7 online), supporting the *pdlp5-1* phenotype in *NahG* (i.e., enhanced PD permeability). However, given that PDLP5 alone does not close PD in the absence of SA accumulation, we conclude that PDLP5 or SA cannot work alone but rather both are required to close PD. In the case of *npr1*, the level of SA and/or PDLP5 must still be above the threshold required for maintaining basal PD callose accumulation/permeability. The fact that basal PD callose/per-meability is abolished in both *NahG* and *pdlp5-1* (Figures 2C and 3D) but not in *npr1* is consistent with our conclusion that basal PD regulation requires PDLP5 only in conjunction with SA but not NPR1.

SA-Induced PD Callose Accumulation via Specific Callose Synthases?

Callose accumulation in planta is induced in response to fungal infection at the penetration site, upon elicitor treatment and bacterial infection, and by other developmental or mechanical factors (Jacobs et al., 2003; Nishimura et al., 2003; DebRoy et al., 2004; Xie et al., 2011). How might SA pathways and PDLP5 specifically affect PD callose accumulation? SA has been implicated in upregulating a subset of *Arabidopsis* callose synthase (CALS) transcripts in an NPR1-dependent manner (Dong et al., 2008). It is tempting to speculate that the loss of PD callose in *PDLP5npr1* is due to the lack of expression of the same NPR1-dependent *CALS* genes, *CALS1/GSL6* and *CALS12/GSL5/PMR4*, described by Dong et al. (2008). How-ever, knocking down those *CALS* genes by RNA interference was reported earlier not to affect callose accumulation either at the cell plate or PD (Jacobs et al., 2003; Nishimura et al., 2003), eliminating the possibility that these isoforms are involved in PD callose deposition. Increases in *CALS* transcript levels may not necessarily correlate with upregulation of callose synthase activity because callose synthase requires additional protein components to form an active complex and other factors for catalytic activation (Brownfield et al., 2009). Also, callose de-position is regulated by the balance between callose synthase and hydrolase activities (Beffa et al., 1996; Levy et al., 2007; Zavaliev et al., 2011); thus, the role of β-1,3-glucanses would need to be taken into consideration.

Recently, two *Arabidopsis CALS* genes, *CALS10/GSL8* and *CALS3/GSL12*, were shown to affect PD callose accu-mulation and play important roles during plant development (Guseman et al., 2010; Vatén et al., 2011). The loss-of-function mutant of *CALS10/GSL8*, *chor*, is compromised for callose deposition at the cell plate, cell wall, and PD and is seedling lethal. Knocking out *CALS3/GSL12* did not alter the level of PD callose deposition, but gain-of-function muta-tions caused hyperaccumulation of PD callose in root cells. Another isoform, *CALS7/GSL7*, was shown to be specifically expressed in phloem and required for both basal and wound-induced callose deposition at the sieve plates (Xie et al., 2011). Collectively, these data suggest that specific *CALS* genes may be responsible for PD callose deposition in cer-tain tissues in specific developmental stages and/or in re-sponse to physiological cues or environmental challenges. In this study, we showed that direct application of SA to *Arabidopsis* leaves induces a substantial amount of PD cal-lose, which suggests that the PD callose induction by bac-terial infection that we previously reported (Lee et al., 2011) is likely mediated through elevated SA concentration. In addition, the hyperaccumulation of PD callose induced by *PDLP5* overexpression was suppressed in *npr1*, under-scoring the critical role of this component (Figure 6). Cur-rently, we are investigating which CALS/hydrolases might be responsible for SA-induced PD callose accumulation during immune responses and the mechanisms by which they may regulate both basal and induced PD permeability in plants.

Crosstalk between Defense Signaling and PD Regulation via PDLP5

Based upon the results presented in this study, we propose a model illustrating how PDLP5 is integrated into the defense signaling cascade to regulate cell-to-cell connectivity in *Arabi-dopsis* (Figure 7). Bacterial pathogen infection activates the basal immune pathway through EDS1 and ICS1, stimulating SA biosynthesis, which leads to the upregulation of *PDLP5* gene expression, which is partially dependent upon NPR1. However, the high expression of PDLP5 also triggers a feedback loop through the same pathway, soon causing a hyperaccumulation of SA in the tissue, which reinforces the defense response. What happens next will require further exploration to gather essential details, but from the experimental evidence that we have at hand so far, PD closure during an SA-based defense response ab-solutely requires both NPR1 and PDLP5. Since it is highly un-likely that NPR1 and PDLP5 interact directly, there is probably an NPR1-dependent "factor X" that must work together with PDLP5 for proper PD callose accumulation and closure during SA-dependent defense. Further biochemical characterization of PDLP5 and identification of the genes that are responsible for the PD callose deposition during immune responses should provide insight into the mechanism by which the restriction of PD is achieved during basal immunity.

METHODS

Plant Materials and Growth Conditions

Seeds of the *Arabidopsis thaliana* mutants *eds1-2*, *ics1*, and *npr1-1* were provided by the H. Bais lab (University of Delaware) and transgenic *NahG* seeds from the X. Dong lab (Duke University). Plants were grown in soil in a 22°C, 60% humidity, 16/8-h-light/dark growth chamber. Crosses were made by removing the sepals, petals, and immature stamens from an unopened bud of an SA pathway mutant and then coating the stigma with pollen from either *PDLP5* or *pdlp5-1* plants. Segregating F2 seeds from the offspring of the crosses were screened with specific primers for each mutant (see Supplemental Table 1 online) using RT-PCR (see section below), and F3 seeds used in this study were collected from double homozygous mutants.

Genomic and RT-PCR

Total genomic DNA was isolated using DNA extraction buffer containing 200 mM Tris-HCl, pH 8.0, 250 mM NaCl, 25 mM EDTA, pH 8.0, and 0.5% SDS, followed by isopropanol precipitation. Genomic DNA resuspended with nano-water was treated with 10 µg/mL RNase A solution (Sigma-Aldrich) at 65°C for 15 min, and 100 to 300 ng DNA was used as template per PCR. Total RNAs were isolated using the Trizol (Invitrogen) method for RT: RNAs were first treated with 2 units of DNaseI (New England Biolabs) for 20 min at 37°C, and 1 µg of each RNA sample was used in a 20 µL total RT reaction containing 0.5 mM deoxynucleotide triphosphate, 0.5 µg oligo(dT), 20 units of Murine RNase inhibitor (NEB), and 20 units of M-MuLV reverse transcriptase (NEB) at 42°C for 1 h. One-twentieth of the cDNAs from RT was used per PCR reaction as follows. Both genomic and RT-PCRs were performed in a 25-µL reaction volume using gene-specific primers (see Supplemental Table 1 online) and *Taq* DNA polymerase (GenScript). All PCRs were performed using a Bio-Rad DNA Engine Peltier thermal cycler. The genomic PCR amplification profile was three cycles of 94°C for 1 min, 52°C for 2 min, and 72°C for 6 min followed by 25 cycles of 94°C for 1 min, 60°C for 2 min, and 72°C for 6 min. The RT-PCR profile was 28 cycles of 94°C for 30 s, 55°C for 45 s, and 72°C for 35 s. Samples were resolved in ethidium bromide–stained 1% agarose gels and visualized and imaged with an Alpha-Imager HP, followed by densitometric quantification using the Image J-NIH program. At least three biological and three technical repeats were performed per sample for quantification.

Confocal Microscopy Imaging, DANS Assay, and Callose Quantification

Plant samples were imaged on a Zeiss AxioObserver inverted light microscope using an LSM 510 META scanhead on a Zeiss LSM 5 LIVE DUO confocal microscope as described before (Lee et al., 2011). Dye loading assays and callose staining were performed on fourth and fifth rosette leaves of 3-week-old plants as described previously (Lee et al., 2011) in the presence or absence of chemical treatments. Briefly, a droplet of 1 mM 5(6)-carboxyfluorescein diacetate (CFDA) was loaded on the adaxial leaf surface of intact *Arabidopsis* plants for 5 min, followed by removal of dye by pipetting and imaging the abaxial leaf surface under a Fluar ×5/0.25 objective lens, using 488-nm laser excitation with a 505- to 550-nm band-pass emission filter. Aniline blue stains were detected using a C-Apochromat ×40/1.20-W Korr UV-VIS-IR objective and 405-nm laser excitation with a 420- to 480-nm band-pass emission filter. For the effect of bacterial infection, dye loading assays and callose staining were performed on systemic rosette leaves (fourth and fifth) 24 h after infection by bacterial infiltration on lower leaves.

Chemical Treatments, Bacterial Infection, and SA Measurement

For SA and catechol treatments, 3-week-old plants grown in soil were sprayed with 100 µM SA, BTH, or catechol dissolved in double-distilled water containing 0.01% Silwet-77 or 10 mM MES, pH 5.8, and samples were collected 24 h after treatment. *Pma ES4326* infection was performed as described before (Lee et al., 2011). Briefly, 3- to 4-week-old *Arabidopsis* plants were infected by infiltration (OD_{600} = 0.001) and incubated for 2 d before DANS and callose quantification assays. Statistical difference between samples was analyzed using a *t* test at $P < 0.001$ or analysis of variance (ANOVA) in conjunction with Fisher's LSD test.

Total SA content was measured by HPLC analysis using 25-d-old plant extracts according to Wang et al. (2011). Briefly, 100 to 200 mg of whole plant tissues was extracted with methanol, dried, and resuspended in 500 µL of 100 mM sodium acetate, pH 5.5. For total SA measurement, 40 units of β-glucosidase (Sigma-Aldrich G-0395) were added to a set of duplicated tubes to digest glucosyl-conjugated SA for 1.5 h at 37°C. All

samples were precipitated with an equal volume of 10% TCA and centrifuged at 10,000*g* for 10 min. The supernatant was further extracted twice with 1 mL of extraction solvent (ethylacetate:cyclopentane:2-propanol 100:99:1, v/v). The top phase was collected and dried in a fume hood overnight. The residual fraction was resuspended in 0.5 mL of 55% methanol by vortex, filtrated through a 0.2-mm nylon spin-prep membrane (Fisher 07-200-389), and subjected to reverse-phase HPLC analysis using an RF2000 fluorescence detector.

Accession Numbers

DNA sequence data from this article can be found in the GenBank/EMBL database under accession numbers AT1G70690, AT1G74710, AT3G48090, AT1G64280, and X83926.1.

Supplemental Data

The following materials are available in the online version of this article.

   Supplemental Figure 1. DANS Assays on Mock- or SA-Treated Wild-Type Col-0 Plants.

   Supplemental Figure 2. SA Treatment for 24 or 48 h Does Not Induce Microlesion Formation.

   Supplemental Figure 3. Confocal Images Showing Adaxial Leaf Surfaces 5 min after Loading with Fluorescent Dye in DANS Assays.

   Supplemental Figure 4. Genotyping and Marker Gene Phenotyping to Confirm Mutations in Desired Genes and Homozygosity of Crosses.

   Supplemental Figure 5. PD Closure Response in *PDLP5ics1* and *PDLP5eds1* Plants upon 100 µM SA Treatment.

   Supplemental Figure 6. SA Treatment Has No Effect on PDLP5 Subcellular Localization.

   Supplemental Figure 7. RT-PCR Showing the Relative Expression Level of *PDLP5*.

   Supplemental Table 1. PCR Primers.

AUTHOR CONTRIBUTIONS

X.W., R.S., W.C., and C.Z. performed research. X.W., R.S., H.L., and J.-Y.L. analyzed the data. J.-Y.L. directed the research and wrote the article.

REFERENCES

Aarts, N., Metz, M., Holub, E., Staskawicz, B.J., Daniels, M.J., and Parker, J.E. (1998). Different requirements for EDS1 and NDR1 by disease resistance genes define at least two R gene-mediated

signaling pathways in *Arabidopsis*. Proc. Natl. Acad. Sci. USA **95:** 10306–10311.

Beffa, R.S., Hofer, R.M., Thomas, M., and Meins, F., Jr.,. (1996). Decreased susceptibility to viral disease of [beta]-1,3-glucanase-deficient plants generated by antisense transformation. Plant Cell **8:** 1001–1011.

Benitez-Alfonso, Y., Faulkner, C., Ritzenthaler, C., and Maule, A.J. (2010). Plasmodesmata: Gateways to local and systemic virus infection. Mol. Plant Microbe Interact. **23:** 1403–1412.

Bilska, A., and Sowinski, P. (2010). Closure of plasmodesmata in maize (*Zea mays*) at low temperature: A new mechanism for inhibition of photosynthesis. Ann. Bot. (Lond.) **106:** 675–686.

Blackman, L.M., and Overall, R.L. (2001). Structure and function of plasmodesmata. Aust. J. Plant Physiol. **28:** 709–727.

Blanco, F., Garretón, V., Frey, N., Dominguez, C., Pérez-Acle, T., Van der Straeten, D., Jordana, X., and Holuigue, L. (2005). Identification of NPR1-dependent and independent genes early induced by salicylic acid treatment in *Arabidopsis*. Plant Mol. Biol. **59:** 927–944.

Brodersen, P., Malinovsky, F.G., Hématy, K., Newman, M.A., and Mundy, J. (2005). The role of salicylic acid in the induction of cell death in *Arabidopsis* acd11. Plant Physiol. **138:** 1037–1045.

Brownfield, L., Doblin, M., Fincher, G., and Basic, A. (2009). Biochemical and molecular properties of biosynthetic enzymes for (1,3)-β-glucans in embryophytes, chlorophytes and rhodophytes. In Chemistry, Biochemistry, and Biology of (1,3)-β-Glucans and Related Polysaccahrides, A. Basic, ed (New York: Academic Press), pp. 283–327.

Burch-Smith, T.M., Stonebloom, S., Xu, M., and Zambryski, P.C. (2011). Plasmodesmata during development: Re-examination of the importance of primary, secondary, and branched plasmodesmata structure versus function. Protoplasma **248:** 61–74.

Burch-Smith, T.M., and Zambryski, P.C. (2010). Loss of INCREASED SIZE EXCLUSION LIMIT (ISE)1 or ISE2 increases the formation of secondary plasmodesmata. Curr. Biol. **20:** 989–993.

Burch-Smith, T.M., and Zambryski, P.C. (2012). Plasmodesmata paradigm shift: Regulation from without versus within. Annu. Rev. Plant Biol. **63:** 239–260.

Cao, H., Bowling, S.A., Gordon, A.S., and Dong, X. (1994). Characterization of an *Arabidopsis* mutant that is nonresponsive to inducers of systemic acquired resistance. Plant Cell **6:** 1583–1592.

Cilia, M.L., and Jackson, D. (2004). Plasmodesmata form and function. Curr. Opin. Cell Biol. **16:** 500–506.

Coll, N.S., Epple, P., and Dangl, J.L. (2011). Programmed cell death in the plant immune system. Cell Death Differ. **18:** 1247–1256.

DebRoy, S., Thilmony, R., Kwack, Y.B., Nomura, K., and He, S.Y. (2004). A family of conserved bacterial effectors inhibits salicylic acid-mediated basal immunity and promotes disease necrosis in plants. Proc. Natl. Acad. Sci. USA **101:** 9927–9932.

Delaney, T.P., Uknes, S., Vernooij, B., Friedrich, L., Weymann, K., Negrotto, D., Gaffney, T., Gut-Rella, M., Kessmann, H., Ward, E., and Ryals, J. (1994). A central role of salicylic acid in plant disease resistance. Science **266:** 1247–1250.

Dempsey, D.A., Vlot, A.C., Wildermuth, M.C., and Klessig, D.F. (2011). Salicylic acid biosynthesis and metabolism. The Arabidopsis Book **9:** e0156, doi/10.1199/tab.0156.

Dong, X., Hong, Z., Chatterjee, J., Kim, S., and Verma, D.P. (2008). Expression of callose synthase genes and its connection with Npr1 signaling pathway during pathogen infection. Planta **229:** 87–98.

Ehlers, K., and Kollmann, R. (1996). Formation of branched plasmodesmata in regenerating *Solanum nigrum* protoplasts. Planta **199:** 126–138.

Ehlers, K., and Kollmann, R. (2001). Primary and secondary plasmodesmata: Structure, origin, and functioning. Protoplasma **216:** 1–30.

Ehlers, K., and van Bel, A.J.E. (2010). Dynamics of plasmodesmal connectivity in successive interfaces of the cambial zone. Planta **231:** 371–385.

Faulkner, C., Akman, O.E., Bell, K., Jeffree, C., and Oparka, K. (2008). Peeking into pit fields: A multiple twinning model of secondary plasmodesmata formation in tobacco. Plant Cell **20:** 1504–1518.

Ferrari, S., Plotnikova, J.M., De Lorenzo, G., and Ausubel, F.M. (2003). *Arabidopsis* local resistance to *Botrytis cinerea* involves salicylic acid and camalexin and requires EDS4 and PAD2, but not SID2, EDS5 or PAD4. Plant J. **35:** 193–205.

Fitzgibbon, J., Beck, M., Zhou, J., Faulkner, C., Robatzek, S., and Oparka, K. (2013). A developmental framework for complex plasmodesmata formation revealed by large-scale imaging of the *Arabidopsis* leaf epidermis. Plant Cell **25:** 57–70.

Fu, Z.Q., and Dong, X. (2013). Systemic acquired resistance: Turning local infection into global defense. Annu. Rev. Plant Biol. **64:** 839–863.

Fu, Z.Q., Yan, S., Saleh, A., Wang, W., Ruble, J., Oka, N., Mohan, R., Spoel, S.H., Tada, Y., Zheng, N., and Dong, X. (2012). NPR3 and NPR4 are receptors for the immune signal salicylic acid in plants. Nature **486:** 228–232.

Gunning, B.E.S. (1978). Age-related and origin-related control of numbers of plasmodesmata in cell-walls of developing *Azolla* roots. Planta **143:** 181–190.

Guseman, J.M., Lee, J.S., Bogenschutz, N.L., Peterson, K.M., Virata, R.E., Xie, B., Kanaoka, M.M., Hong, Z.L., and Torii, K.U. (2010). Dysregulation of cell-to-cell connectivity and stomatal patterning by loss-of-function mutation in *Arabidopsis chorus* (*glucan synthase-like 8*). Development **137:** 1731–1741.

Heck, S., Grau, T., Buchala, A., Métraux, J.P., and Nawrath, C. (2003). Genetic evidence that expression of NahG modifies defence pathways independent of salicylic acid biosynthesis in the *Arabidopsis-Pseudomonas syringae pv. tomato* interaction. Plant J. **36:** 342–352.

Heinlein, M. (2002). The spread of tobacco mosaic virus infection: Insights into the cellular mechanism of RNA transport. Cell. Mol. Life Sci. **59:** 58–82.

Hou, S., Yang, Y., and Zhou, J.M. (2009). The multilevel and dynamic interplay between plant and pathogen. Plant Signal. Behav. **4:** 283–293.

Jacobs, A.K., Lipka, V., Burton, R.A., Panstruga, R., Strizhov, N., Schulze-Lefert, P., and Fincher, G.B. (2003). An *Arabidopsis* callose synthase, GSL5, is required for wound and papillary callose formation. Plant Cell **15:** 2503–2513.

Jagadeeswaran, G., Raina, S., Acharya, B.R., Maqbool, S.B., Mosher, S.L., Appel, H.M., Schultz, J.C., Klessig, D.F., and Raina, R. (2007). *Arabidopsis* GH3-LIKE DEFENSE GENE 1 is required for accumulation of salicylic acid, activation of defense responses and resistance to *Pseudomonas syringae*. Plant J. **51:** 234–246.

Koh, E.J., Zhou, L., Williams, D.S., Park, J., Ding, N., Duan, Y.P., and Kang, B.H. (2012). Callose deposition in the phloem plasmodesmata and inhibition of phloem transport in citrus leaves infected with "*Candidatus Liberibacter asiaticus*". Protoplasma **249:** 687–697.

Lawton, K., Weymann, K., Friedrich, L., Vernooij, B., Uknes, S., and Ryals, J. (1995). Systemic acquired resistance in *Arabidopsis* requires salicylic acid but not ethylene. Mol. Plant Microbe Interact. **8:** 863–870.

Lee, J.Y., and Lu, H. (2011). Plasmodesmata: The battleground against intruders. Trends Plant Sci. **16:** 201–210.

Lee, J.Y., Wang, X., Cui, W., Sager, R., Modla, S., Czymmek, K., Zybaliov, B., van Wijk, K., Zhang, C., Lu, H., and Lakshmanan, V. (2011). A plasmodesmata-localized protein mediates crosstalk between cell-to-cell communication and innate immunity in *Arabidopsis*. Plant Cell **23:** 3353–3373.

Lee, M.W., Jelenska, J., and Greenberg, J.T. (2008). *Arabidopsis* proteins important for modulating defense responses to *Pseudomonas syringae* that secrete HopW1-1. Plant J. **54:** 452–465.

Levy, A., Erlanger, M., Rosenthal, M., and Epel, B.L. (2007). A plasmodesmata-associated beta-1,3-glucanase in *Arabidopsis*. Plant J. **49:** 669–682.

Lorrain, S., Vailleau, F., Balagué, C., and Roby, D. (2003). Lesion mimic mutants: Keys for deciphering cell death and defense pathways in plants? Trends Plant Sci. **8:** 263–271.

Lucas, W.J., Ham, B.K., and Kim, J.Y. (2009). Plasmodesmata - Bridging the gap between neighboring plant cells. Trends Cell Biol. **19:** 495–503.

Lucas, W.J., and Lee, J.Y. (2004). Plasmodesmata as a supracellular control network in plants. Nat. Rev. Mol. Cell Biol. **5:** 712–726.

Malamy, J., Carr, J.P., Klessig, D.F., and Raskin, I. (1990). Salicylic acid: A likely endogenous signal in the resistance response of tobacco to viral infection. Science **250:** 1002–1004.

Maule, A.J. (2008). Plasmodesmata: Structure, function and biogenesis. Curr. Opin. Plant Biol. **11:** 680–686.

Maule, A.J., Benitez-Alfonso, Y., and Faulkner, C. (2011). Plasmodesmata - Membrane tunnels with attitude. Curr. Opin. Plant Biol. **14:** 683–690.

Mur, L.A., Kenton, P., Lloyd, A.J., Ougham, H., and Prats, E. (2008). The hypersensitive response; the centenary is upon us but how much do we know? J. Exp. Bot. **59:** 501–520.

Nawrath, C., and Métraux, J.P. (1999). Salicylic acid induction-deficient mutants of *Arabidopsis* express PR-2 and PR-5 and accumulate high levels of camalexin after pathogen inoculation. Plant Cell **11:** 1393–1404.

Nishimura, M.T., Stein, M., Hou, B.H., Vogel, J.P., Edwards, H., and Somerville, S.C. (2003). Loss of a callose synthase results in salicylic acid-dependent disease resistance. Science **301:** 969–972.

Oparka, K.J., and Roberts, A.G. (2001). Plasmodesmata. A not so open-and-shut case. Plant Physiol. **125:** 123–126.

Ormenese, S., Bernier, G., and Périlleux, C. (2006). Cytokinin application to the shoot apical meristem of *Sinapis alba* enhances secondary plasmodesmata formation. Planta **224:** 1481–1484.

Ormenese, S., Havelange, A., Bernier, G., and van der Schoot, C. (2002). The shoot apical meristem of *Sinapis alba* L. expands its central symplasmic field during the floral transition. Planta **215:** 67–78.

Ormenese, S., Havelange, A., Deltour, R., and Bernier, G. (2000). The frequency of plasmodesmata increases early in the whole shoot apical meristem of *Sinapis alba L.* during floral transition. Planta **211:** 370–375.

Pouwels, J., Kornet, N., van Bers, N., Guighelaar, T., van Lent, J., Bisseling, T., and Wellink, J. (2003). Identification of distinct steps during tubule formation by the movement protein of Cowpea mosaic virus. J. Gen. Virol. **84:** 3485–3494.

Pouwels, J., van der Velden, T., Willemse, J., Borst, J.W., van Lent, J., Bisseling, T., and Wellink, J. (2004). Studies on the origin and structure of tubules made by the movement protein of Cowpea mosaic virus. J. Gen. Virol. **85:** 3787–3796.

Radford, J.E., Vesk, M., and Overall, R.L. (1998). Callose deposition at plasmodesmata. Protoplasma **201:** 30–37.

Rietz, S., Stamm, A., Malonek, S., Wagner, S., Becker, D., Medina-Escobar, N., Vlot, A.C., Feys, B.J., Niefind, K., and Parker, J.E. (2011). Different roles of Enhanced Disease Susceptibility1 (EDS1) bound to and dissociated from Phytoalexin Deficient4 (PAD4) in *Arabidopsis* immunity. New Phytol. **191:** 107–119.

Rinne, P.L.H., and van der Schoot, C. (2003). Plasmodesmata at the crossroads between development, dormancy, and defense. Can. J. Bot. **81:** 1182–1197.

Rinne, P.L.H., Welling, A., Vahala, J., Ripel, L., Ruonala, R., Kangasjärvi, J., and van der Schoot, C. (2011). Chilling of dormant buds hyperinduces FLOWERING LOCUS T and recruits GA-inducible 1,3-beta-glucanases to reopen signal conduits and release dormancy in *Populus*. Plant Cell **23:** 130–146.

Rivas-San Vicente, M., and Plasencia, J. (2011). Salicylic acid beyond defence: Its role in plant growth and development. J. Exp. Bot. **62:** 3321–3338.

Robards, A.W., and Lucas, W.J. (1990). Plasmodesmata. Annu. Rev. Plant Physiol. **41:** 369–419.

Roberts, A.G., and Oparka, K.J. (2003). Plasmodesmata and the control of symplastic transport. Plant Cell Environ. **26:** 103–124.

Rustérucci, C., Aviv, D.H., Holt III, B.F., Dangl, J.L., and Parker, J.E. (2001). The disease resistance signaling components EDS1 and PAD4 are essential regulators of the cell death pathway controlled by LSD1 in *Arabidopsis*. Plant Cell **13:** 2211–2224.

Ryals, J.A., Neuenschwander, U.H., Willits, M.G., Molina, A., Steiner, H.Y., and Hunt, M.D. (1996). Systemic acquired resistance. Plant Cell **8:** 1809–1819.

Schoelz, J.E., Harries, P.A., and Nelson, R.S. (2011). Intracellular transport of plant viruses: Finding the door out of the cell. Mol. Plant **4:** 813–831.

Seagull, R.W. (1983). Differences in the frequency and disposition of plasmodesmata resulting from root cell elongation. Planta **159:** 497–504.

Sevilem, I., Miyashima, S., and Helariutta, Y. (2013). Cell-to-cell communication via plasmodesmata in vascular plants. Cell Adhes. Migr. **7:** 27–32.

Shah, J. (2009). Plants under attack: Systemic signals in defence. Curr. Opin. Plant Biol. **12:** 459–464.

Simpson, C., Thomas, C., Findlay, K., Bayer, E., and Maule, A.J. (2009). An *Arabidopsis* GPI-anchor plasmodesmal neck protein with callose binding activity and potential to regulate cell-to-cell trafficking. Plant Cell **21:** 581–594.

Spoel, S.H., and Dong, X. (2012). How do plants achieve immunity? Defence without specialized immune cells. Nat. Rev. Immunol. **12:** 89–100.

Tada, Y., Spoel, S.H., Pajerowska-Mukhtar, K., Mou, Z., Song, J., Wang, C., Zuo, J., and Dong, X. (2008). Plant immunity requires conformational changes [corrected] of NPR1 via S-nitrosylation and thioredoxins. Science **321:** 952–956.

Thomas, C.L., Bayer, E.M., Ritzenthaler, C., Fernandez-Calvino, L., and Maule, A.J. (2008). Specific targeting of a plasmodesmal protein affecting cell-to-cell communication. PLoS Biol. **6:** e7.

Ueki, S., and Citovsky, V. (2011). To gate, or not to gate: Regulatory mechanisms for intercellular protein transport and virus movement in plants. Mol. Plant **4:** 782–793.

van Lent, J., Storms, M., van der Meer, F., Wellink, J., and Goldbach, R. (1991). Tubular structures involved in movement of *cowpea mosaic virus* are also formed in infected cowpea protoplasts. J. Gen. Virol. **72:** 2615–2623.

van Wees, S.C., and Glazebrook, J. (2003). Loss of non-host resistance of *Arabidopsis* NahG to *Pseudomonas syringae pv. phaseolicola* is due to degradation products of salicylic acid. Plant J. **33:** 733–742.

Vatén, A., et al. (2011). Callose biosynthesis regulates symplastic trafficking during root development. Dev. Cell **21:** 1144–1155.

Vlot, A.C., Dempsey, D.A., and Klessig, D.F. (2009). Salicylic acid, a multifaceted hormone to combat disease. Annu. Rev. Phytopathol. **47:** 177–206.

Vogelmann, K., Drechsel, G., Bergler, J., Subert, C., Philippar, K., Soll, J., Engelmann, J.C., Engelsdorf, T., Voll, L.M., and Hoth, S. (2012). Early senescence and cell death in *Arabidopsis* saul1 mutants involves the PAD4-dependent salicylic acid pathway. Plant Physiol. **159:** 1477–1487.

Waigmann, E., Lucas, W.J., Citovsky, V., and Zambryski, P. (1994). Direct functional assay for tobacco mosaic virus cell-to-cell

movement protein and identification of a domain involved in increasing plasmodesmal permeability. Proc. Natl. Acad. Sci. USA **91:** 1433–1437.

Wang, D., Weaver, N.D., Kesarwani, M., and Dong, X. (2005). Induction of protein secretory pathway is required for systemic acquired resistance. Science **308:** 1036–1040.

Wang, G.F., Seabolt, S., Hamdoun, S., Ng, G., Park, J., and Lu, H. (2011). Multiple roles of WIN3 in regulating disease resistance, cell death, and flowering time in *Arabidopsis*. Plant Physiol. **156:** 1508–1519.

Wiermer, M., Feys, B.J., and Parker, J.E. (2005). Plant immunity: The EDS1 regulatory node. Curr. Opin. Plant Biol. **8:** 383–389.

Wildermuth, M.C., Dewdney, J., Wu, G., and Ausubel, F.M. (2001). Isochorismate synthase is required to synthesize salicylic acid for plant defence. Nature **414:** 562–565.

Wille, A.C., and Lucas, W.J. (1984). Ultrastructural and histochemical studies on guard cells. Planta **160:** 129–142.

Xie, B., Wang, X., Zhu, M., Zhang, Z., and Hong, Z. (2011). CalS7 encodes a callose synthase responsible for callose deposition in the phloem. Plant J. **65:** 1–14.

Zavaliev, R., Ueki, S., Epel, B.L., and Citovsky, V. (2011). Biology of callose (β-1,3-glucan) turnover at plasmodesmata. Protoplasma **248:** 117–130.